in vivo *26*: 271-276 (2012)

Cardiovascular Prosthetic Surgery: An Analysis of Cellular and Molecular Patterns Underlying Valve Implantation Failure

GENNARO MAZZARELLA[1], ANDREA BIANCO[2], ANGELA LUCARIELLO[3], LEONILDE SAVARESE[3], ANGELAMARIA FIUMARELLA[3], FLAVIO CERASUOLO[4], FRANCA FERRARACCIO[5] and ANTONIO DE LUCA[3]

[1]*Department of Cardiothoracic and Respiratory Sciences, Second University of Naples, Naples, Italy;*
[2]*Department of Health Sciences, Faculty of Medicine and Surgery, University of Molise, Naples, Italy;*
[3]*Department of Medicine and Public Health, Section of Human Anatomy, Second University of Naples, Naples, Italy;*
[4]*Monaldi Hospital, Department of Cardiosurgery, Naples, Italy;*
[5]*Department of Medicine and Public Health, Section of Pathologic Anatomy, Second University of Naples, Naples, Italy*

Abstract. *Cardiac valves have a very complex microscopic architecture, this is due to the presence of many cell types and to the variegated stroma. From a morphological point of view, both physiological and pathological processes clearly show there to be an anatomic continuity between valve leaflets and perivalvular tissues; indeed, both component should be taken into consideration during thrombotic processes and in fibrous tissue formation. At present, morphological features are well known and classified, while little is known about histogenetic features: fibrous tissue formation and the role of the various types of adhesion molecules and cells which participate in this process still have to be fully elucidated. In the current study, we focused on the histological analysis of the pannus. In particular, we demonstrated that the true connective nature of the exuberant fibrous tissue was entirely composed of collagen/fibronectin fibre bundles and fibroblasts. Moreover we observed that the phlogistic infiltrates were composed of immune cells, mainly represented by $CD4^+$ and $CD8^+$ T lymphocytes. Finally we also tried to assess not only the degree of endothelial layer loss, but also the extent of revascularization in the exuberant fibrous tissue.*

Cardiac valves have a very complex microscopic architecture due to the presence of many types of cells, as well as to the variable stromal pattern, involving intercellular matrix and bioactive molecules. From a morphological point of view, both physiological and pathological processes clearly demonstrate an anatomic continuity between valve leaflets and perivalvular tissues; this anatomical feature is common to mechanical and biological prosthetic valves and leads to an involvement of both valves and perivalvular tissues in thrombotic processes and in fibrous tissue formation. Thrombotic and fibrotic outcomes are similar in use of the two prosthetic types, although a more frequent and early risk of thrombosis has been reported in cases where mechanical valves were employed (1-4).

The processes of thrombus and pannus (a fibrous cloth) formation can take place separately, or one can be the consequence of the other: in fact, the fibroid tissue can, even if not frequently, be the etiological factor for thrombus formation (2). Regarding histogenetic and morphological features of pannus, it is well known that it develops on prosthetic valves, starting from the valvular periannulus (5-7).

At present, morphological features are well known and classified, while little is known about histogenetic features: fibrous tissue formation and the role of the various types of adhesion molecules and cells which participate in this process still have to be fully elucidated. Not only are the biopathological processes of cardiac valves and perivalvular tissues are still poorly understood, but so are also their responses in terms of cell recruitment to various pathological and injurious conditions (8, 9).

Due to the complexity of such histogenetic processes many hypotheses have been proposed concerning the role of the different cell types. With regard to the pannus, numerous questions still remain concerning the biological and histomorphological roles of cells and mediators involved in its formation. A more extensive quantitative and comparative analysis could possibly clarify the critical role played by cellular and molecular components in the histogenesis of the pannus.

In the current study, we focused on the histological analysis of the pannus. In particular, we wanted not only to determine the nature of the exuberant fibrous tissue, but also to

Correspondence to: Dr. Antonio De Luca, MD, Ph.D., Department of Medicine and Public Health, Section of Human Anatomy, Second University of Naples, Via L. Armanni 5, 80138 Naples, Italy. e-mail: antonio.deluca@unina2.it

Key Words: Cardiac valves, perivalvular tissues, inflammation, cardiovascular prostheric surgery.

understand the exact composition of the local cell population, with regard to the cluster of differentiation 4 and 8 of T-cells ($CD4^+$ and $CD8^+$). We also tried to assess the degree of endothelial layer loss and the extent of revascularization in the exuberant fibrous tissue.

Materials and Methods

The investigation carried out here conforms with the principles outlined in the Declaration of Helsinki.

Surgical procedures. In the Cardiac Surgery Ward of the Monaldi Hospital, 118 patients underwent cardiac surgery in the last five years. Fifty-nine of them (50%) underwent valve surgery as follows: forty-nine (41.5%) underwent primitive valve replacement; three (2.5%) were re-operated on because they had developed prosthetic thrombosis; the remaining seven (5.9%) were re-operated on due to prosthetic dysfunctions of the type of exuberant pannus. Among the seven patients displaying prosthetic dysfunctions, six were females, with an average age of 60.6±10.32 (age ranging from 49 to 73 years). There was only one single 59-year old male patient, which let us to hypothesize that this kind of dysfunction might have a greater incidence (85.7%) in the female sex.

Mitral prosthetic valve malfunctioning was present in six cases and aortic prosthetic valve impairment was present in one case. The average time between first and second cardiac valve surgery was 13.14±8.09 (S.D.) years, with a minimum of 3 years and a maximum of 25 years. Malfunctioning prostheses that needed replacement were of the following type: ball type (Starr-Edwards) in three cases; bi-disc type (Edwards-Mira) in two cases; mono-disc type (Sorin) in one case; a bio-prosthesis (SJM) in the remaining case.

Replacement prostheses implanted were the following: five bi-disc (Edwards-Mira); one ball-type (Starr-Edwards) in the patient who already had received the same kind of prosthesis; another ball-type prosthesis was adopted in a patient previously treated with a bio-prosthesis who could no longer tolerate permanent anticlotting therapy due to thrombocytopenia.

Forty minutes before anaesthesia, a peripheral venous blood sample was taken from each patient and collected in a BD vacutainer containing 0.073 ml of K3EDTA, and used for CD4/CD8 ratio assessment, which would later be correlated to that obtained from the analysis of prosthetic tissue. Surgical access was always gained through median sternotomy followed by aortic/atrio-caval cannulation (five cases) or bi-caval cannulation (two cases). Extracorporeal circulation (CEC) was performed under moderate hypothermia (30˚C), with aortic clamping and aortic bulb perfusion with cardioplegic solution (10). Average CEC duration was 66 min with a minimum of 60 min and a maximum of 72 min. Left atriotomy or aortotomy were performed to gain access to the mitral and the aortic valves, respectively.

Explanted valvular prostheses were first examined macroscopically in order to verify the presence of prosthetic thrombosis and exuberant pannus; excessive periannular fibrous matter affecting the normal mobility of the prosthesis was removed and placed in 4% w/v buffered formalin.

Histology and immunohistochemistry of valve/pannus samples. All the immunoassays were carried out by a KBMK 750600 automatic immunostainer (Ventana Medical System, Tucson, Arizona, USA). Specimens were fixed in 10% formalin in phosphate buffer (0.1 M, pH 7.4), dehydrated in increasing series of alcool, diaphanized and embedded in Histowax (Carlo Erba, Milan, Italy) resin. Four micrometer thick sections were cut and set up either for normal histological analysis (haematoxylin-eosin or Van Gieson haematoxylin staining) or for immunohistochemical analysis. In latter case, endogenous peroxidase activity was blocked by 10 min incubation in Dako peroxidase blocking reagent (DAKO, Milan, Italy); antigen retrieval was performed by incubating sections for 5 min in target retrieval solution (0.01 M/l citrate buffer pH 6.0) at 100˚C. At this point, primary antibodies [Abs (all from DAKO, Milan, Italy)] were used, directed against fibronectin, smooth-muscle actin, CD34 (class II QBEnd 10), CD8-T *cell* (suppressor/cytotoxic) antigen, CD4-T *cell* (helper/inducer) antigen, CD45 RA-B *cell* antigen, in order to evaluate the collagen and myofibroblastic constituents, and the extent of neovascularization, as well as the degree of endothelium loss, the eventual increase of B- and T-cells also activated as expression of phlogosis. All these aspects were also analysed in peripheral blood samples. CD34 detection only required a further step consisting in the incubation of samples in proteinase K [0.05M proteinase K (Ventana Medical System, Tucson, Arizona, USA) in 15 mM Tris-HCl pH 7.5] prior to anti-CD34 primary Ab use.

In all cases, primary Ab incubation was followed by incubation with streptavidin-biotin peroxidase complex (Ventana Medical System, Tucson, Arizona, USA) [30', at room temperature (RT), in a light-proof, humidified chamber]; then 5 min incubation with 3,3' diaminobenzidine tetrahydrochloride (DAB) in 1× PBS, at RT, in a light-proof, humidified chamber; cell nuclei were then counterstained with Mayer's hematoxylin. Slides were dehydrated in graded ethanol solutions to be finally mounted with Entellan (Merck, Milan, Italy).

For negative control slides, Tris-buffered saline solution was used instead of primary Abs. The presence of newly formed blood vessels of any size was determined through the measurement of the sites and levels of CD34 expression. In particular, microvessels were counted (MVC) and total microvascular area (MVA) was quantified; moreover, we looked for $CD4^+$ and $CD8^+$ T-lymphocytes, which were counted in standardized sample volumes made up from serial sections. Processing and calculations were made with a Leica IMM 500 computerized image analyzer (Leica, Milan, Italy).

Scanning electron microscopy (SEM) analysis. Tissue fragments 0.5mm thick were fixed in 10% buffered formalin pH 7.4 and 100 mOsm, dehydrated in graded concentrations of ethanol, critical point treated for ethanol replacement with liquid CO_2 (38˚C, 85 bar pressure). An Emitech K550 sputtering device (Quorum Technologiee, England) was utilized to coat specimens with a 30mÅ thin gold film. Specimens were finally observed under a Zeiss DSM 940 scanning electron microscope (Zeiss, Milan, Italy).

Lymphocyte separation from whole blood and cytofluorimetric CD4/CD8 ratio assessment. Peripheral blood samples intravenously taken from patients were collected into heparinized glass test tubes. Lymphocytes were then obtained through Ficoll (Amersham Biosciences, Geneve, Suiss) separation. Briefly, blood was put in tubes containing Ficoll in a 2:1 ratio. Tubes were then centrifuged at 2.000 rpm × g for 20 min, lymphocytes collected and resuspended in cold Hank's solution and then centrifuged for a further 20 min still at 2.000 rpm × g. If red blood cells were detected into the lymphocyte pellet, erythrolysis was performed as follows: pellet was incubated in

Table I. *Immunostaning findings in peripheral blood and pannus of individual patients.*

Patient ID	Peripheral blood $CD4^+/CD8^+$ T-cell ratio	$CD34^+$ vessels (n)	CD34 positivity Total Area (μn^2)	Max. unitary area of CD34 positivity (μn^2)	Min. unitary area of CD34 positivity (μn^2)	Mean CD34 area (μn^2)	Bioptic tissue $CD4^+/CD8^+$ T-cell ratio
1	2.2	19	9635.9	2732.93	59.85	507.15	2.5
2	5.0	124	49684.07	14063.62	0.19	400.678	3.5
3	1.5	70	151792.60	22279.65	12.07	2168.47	3.2
4	3.7	62	20032.09	1274.43	0.11	323.09	0.4
5	2.1	n.d.	n.d.	n.d.	n.d.	n.d.	3.0
6	10.0	23	9635.9	6008.82	184.62	1214.31	2.1
7	19.0	57	72238.94	8324.32	74.7	1267.35	3.2

5 ml of 10.2% NaCl for 30", then replaced with 5 ml of a 1.6% NaCl solution; the suspension was then centrifuged at 800 rpm for 15 min. The pellet rinsed with 1× PBS and then re-centrifuged. At the end of this process, then final pellet was resuspended in PBS.

Cell viability was evaluated by Trypan blue exclusion. Purified lymphocytes were incubated with permeabilising solution, then with fluorescent probe-conjugated monoclonal primary antibodies directed against CD3, CD4 and CD8 antigens (DAKO, Milan, Italy) (10 min, in a humidified and light-proof chamber at RT. Pellets were then resuspended in PBS and centrifuged for 5 min at 1.000 rpm with 500µl of 0.1% paraformaldehyde in 1× PBS and thereby cytofluorimetrically analysed for CD3, CD4 and CD8 expression.

Results

A peripheral venous blood sample was collected from each patient and used for evaluation of the expression of CD4, CD8, CD 34 and CD4/CD8 ratio assessment. Table I reports the positive staining for individual patients examined.

Fibronectin expression analysis of valve and pannus specimens revealed a stromal architecture entirely composed of collagen/fibronectin fibre bundles and fibroblasts (Figure 1a). No smooth-muscle actin was detectable, which ruled out the presence of myofibroblasts in the samples. Neovascularization was present in six out of the seven examined cases, being quite noticeable in one case and mid-high in another three other cases (see Table I).

Newly formed capillaries were internally covered by cubical-shaped endothelial cells, appearing quite hypertrophic and protruding the vessel lumen. Their topographical distribution appeared rather even, with no particularly dense area of neovasculature, mainly represented by CD34, with larger vessels typically localized at the deeper stromal area (Figure 1b).

Phlogistic infiltrates were composed of immune cells, mainly represented by $CD4^+$ and $CD8^+$ T lymphocytes (Figure 1c and 1d). The number of these cell elements showed some variability from case to case, possibly due to the variable degree of local phlogosis. Lymphocyte density was found to be mid-high in two cases, very high in one single case, and quite low in the remaining four cases (see Table I).

The degree of endothelial loss, as analysed by CD34 expression, was quite severe in two cases, mild in another two cases (Figure 1e), with almost equally represented superficial areas normally covered by endothelial sheath and other areas rather exhibiting complete absence of endothelial cells; two cases exhibited a relatively low degree of endothelium loss, and only in one case was the endothelial layer normally represented (see Table I).

SEM ultrastructural analysis of the pannus surface confirmed light microscopy findings. The superficial areas of the specimens appeared free from coaguli (Figure 1f) and rather wrinkled or marked by longitudinally arranged thickenings of the fibrous matter (Figure 1g). The endothelial sheet was generally not visible at all. The surface structural pattern described above appeared uniformly represented, being suggestive of massive fibroid transformation. No areas of neovascularization were detected superficially, with newly formed vessels being localized deep inside the pannus (Figure 1h).

Discussion

The overall analysis of the specimens showed that the pannus appeared composed of collagen fibres and fibroblasts, with myofibroblasts always being undetectable, this accounting for no transdifferentiation of mesenchymal cells into myofibroblastic elements. Moreover, the inflammation cell population was entirely represented by T-lymphocytes. This feature is in accordance with *in vitro* studies of immune cells during fibrous tissue histogenesis that had made it possible to identify a fundamental role for T lymphocytes in the immunogenetic processes leading to fibrous tissue formation, so they seem to exert a regulatory effect during proliferative processes involving either interstitial tissues or valvular/perivalvular endothelium (11, 12).

The observation of the specimens showed that the neovascularization and endothelial sheet hypertrophy/hyperplasia were also common findings, although endothelial cells appeared to cover the pannus in a very discontinuous manner, with good portions of the pannus surface area clearly

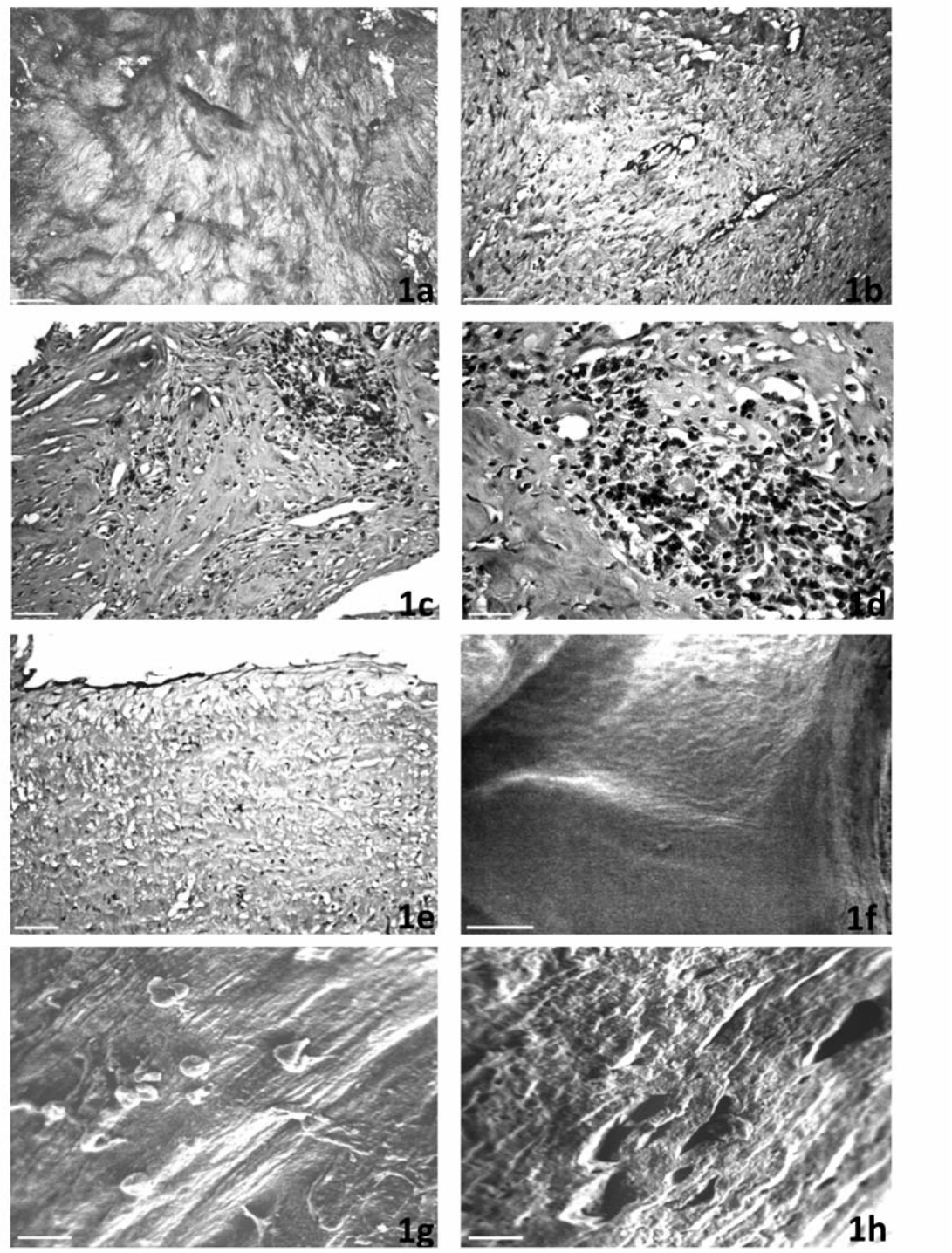

Figure 1. *a: Fibronectin immunostaining of pannus. Note the fibrillary nature of the entire area, with fibronectin positive fibres oriented the same way as (unstained) collagen fibres. Light microscopy; scale bar=250 μm. b: CD34 immunostaining of neovasculature in pannus. Light microscopy; scale bar=150 μm. c: CD4+ T-Cell immunostaining of pannus. Light microscopy; scale bar r=150 μm. d: CD8+ T-Cell immunostaining of pannus. Light microscopy; scale bar=100 μm. e: CD34 immunostaining of pannus. Note the marked CD34 positivity at the top left of the superficial endothelial sheath, which decreases moving to the right, to suddenly disappear at top right of the figure, where endothelial loss appears quite evident. Light microscopy; scale bar=150 μm. f: Superficial appearance of pannus. Only few curved wrinkles are partially evident on the left, at the exact para-annular site. SEM micrograph; scale bar=200 μm. g: Superficial appearance of pannus. Wrinkles and longitudinally arranged thickenings of the fibrous matter are clearly evident. SEM micrograph; scale bar=10 μm. h: Medium and an large-sized newly formed vessels as typically found deep inside specimens of pannus. SEM micrograph; scale bar=10 μm.*

showing total absence of these cell elements. It is possible to correlate the poorness of endothelial cell covering and the severity of the phlogistic events. In fact, a potential role for endothelium in valvular degenerative and inflammatory events has also been raised, and, with regard to cardiovascular disorders, damage of the endothelial layer was showed to lead to phlogosis, intimal hyperplasia, platelet aggregation and vasospasm (13).

It is well recognized that the endothelial layer might play a fundamental role in the histogenesis of valvular and perivalvular lesions, and only a careful analysis of endothelial cells alterations might help in assessing the degree of degenerative and inflammatory processes affecting cardiac valves (14).

It is also important to remember that vascular endothelial growth factor is able to induce the transcriptional factor: Nuclear factor of activated T-cells, cytoplasmic 1 (NFATc1), that is a crucial modulator during valvular wound healing processes (15).

Moreover we observed that interstitial cells exhibited a high degree of proliferation, as one would expect taking into account their active role in reparative processes also taking place after cardiac valve endoprosthesic surgery, in accordance with what has been documented by other authors (16).

Finally, we would like to point out that periannular pannus forming after cardiac valve replacement surgery should be regarded as the morphological expression of a scarring process that initiates at the periannular level to then progressively extend to the entire valve area. Some believe that this event is a consequence of the increase of the proliferation rate presumably due to production of fibroblast-derived growth factors (5).

Acknowledgements

The study was partially supported by the Second University of Naples.

References

1 Vitale N, Renzulli A, Agozzino L, Pollice A, Tedesco N, de Luca Tupputi Schiuosa L and Cotrufo M: Obstruction of mechanical mitral prostheses: analysis of pathologic findings. Ann Thorac Surg *63*: 1101-1116, 1997.

2 Rizzoli G, Guglielmi C, Toscano G, Pistorio V, Vendramin I, Bottio T, Thiene G and Casarotto D: Reoperations for acute prosthetic thrombosis and pannus: an assessment of rates, relationship and risk. Eur J Cardiothorac Surg *16*: 74-80, 1999.

3 Càceres-Lòriga FM, Pérez-Lòpez H, Morlans-Hernàndez K, Facundo-Sànchez H, Santos-Gracia J, Valiente-Mustelier J, Rodiles-Aldana F, Marrero-Mirayaga MA, Betancourt BY and Lòpez-Saura P: Thrombolysis as first choice therapy in prosthetic heart valve thrombosis. A study of 68 patients. J Thromb Thrombolysis *21*: 185-190, 2006.

4 Schoen FJ. Heart valve tissue engineering: Quo vadis? Curr Opin Biotechnol *22*: 698-705, 2011.

5 Teshima H, Hayashida N, Yano H, Nishimi M, Tayama E, Fukunaga S, Akashi H, Kawara T and Aoyagi S: Obstruction of St Jude Medical valves in the aortic position: histology and Immunohistochemistry of pannus. J Thorac Cardiovasc Surg *126*: 401-407, 2003.

6 Hakuno D, Kimura N, Yoshioka M and Fukuda K: Molecular mechanisms underlying the onset of degenerative aortic valve disease. J Mol Med (Berl) *87*: 17-24, 2009.

7 Oda T, Kato S, Tayama E, Fukunaga S, Akashi H and Aoyagi S: Pannus overgrowth after mitral valve replacement with a Carpentier-Edwards pericardial bioprothesis. J Artif Organs 12: 55-57, 2009.

8 Durbin AD and Gotlieb AI: Advances towards understanding heart valve response to injury. Cardiovasc Pathol *11*: 69-77, 2002.

9 Xu S and Grande-Allen KJ: The role of cell biology and leaflet remodelling in the progression of heart valve disease. Methodist Debakey Cardiovasc J *6*: 2-7, 2010.

10 von Oppell UO, Du Toit EF, King LM, Owen P, Dunne T, Reichart B and Opie LH: St. Thomas' Hospital cardioplegic solution. Beneficial effect of glucose and multidose reinfusions of cardioplegic solution. J Thorac Cardiovasc Surg *102(3)*: 405-412, 1991.

11 Batten P, McCormack AM, Rose ML and Yacoub MH: Valve interstitial cells induce donor-specific T-cell anergy. J Thorac Cardiovasc Surg *122*: 129-135, 2001.

12 Bosch JA, Berntson GG, Cacioppo JT, Dhabhar FS and Marucha PT: Acute stress evokes selective mobilization of T-cells that differ in chemokine receptor expression: a potential pathway linking immunologic reactivity to cardiovascular disease. Brain Behav Immun *17*: 251-259, 2003.

13 Zilla P, von Oppell U and Deutsch M: The endothelium: a key to the future. J Card Surg *8*: 32-60, 1993.

14 Leask RL, Jain N and Butany J. Endothelium and valvular diseases of the heart. Microsc Res Tech *60*: 129-137, 2003.

15 Johnson EN, Lee YM, Sander TL, Rabkin E, Schoen FJ, Kaushal S and Bischoff J: NFATc1 mediates vascular endothelial growth factor-induced proliferation of human pulmonary valve endothelial cells. J Biol Chem *278*: 1686-1692, 2003.

16 Gotlieb AI, Rosenthal A and Kazemian P: Fibroblast growth factor 2 regulation of mitral valve interstitial cell repair *in vitro*. J Thorac Cardiovasc Surg *124*: 591-597, 2002.

Received December 1, 2011
Revised January 19, 2012
Accepted January 23, 2012